Laurențiu-Ionuț CRISTEA, Daniel DOBRE

CONCEPTUAL DESIGN AND DEVELOPMENT OF A PARAGLIDER AIRFOIL

Abstract: *The paper presents the design of a paraglider airfoil with superior flight characteristics, which provides safety, comfort and is easy to maintain by the user. The aerodynamics of paraglider airfoil are complex because they involve unstable turbulent three-dimensional airflows over flexible and deformable limits. The main improvement of the paper is the increase of the lift/drag ratio obtained by modifying the aerodynamic profile in the area of the leading edge, according to the "shark nose" model, and adding a reinforced structure in the flight edge to maintain the ideal shape of the aerodynamic profile at different angles of attack. The paper presents aerodynamic calculations, on a lifting surface of the paraglider airfoil that respects the NACA 2412 profile, made with a MathCAD program through which the coordinates of the profile were obtained at any point. The Paratailor 9 software was used to generate the paraglider model. The structural evaluation of the recreational paraglider model that meets the wishes of the current buyers is also presented.*

Key words: *conceptual design, flight characteristics, aerodynamic calculations, paraglider configuration, 3D modeling.*

1. INTRODUCTION

The field of general aviation is constantly evolving both in terms of the technologies currently available and in terms of the number of people it attracts. Thus, more and more people want to own a flying machine that they can use both for recreational purposes and as a means of transportation.

In line with current trends, aerospace technology has been forced to develop sustainable aircraft. Research has shown the need to preserve non-renewable fuels, so the use of electric motors has grown. Consequently, the aim of this paper is to create a paramotor version with superior features for recreational or school instructional flights, incorporating a lightweight modular electric motor and using a small capital, materials and non-harmful energy sources. The aim was also to design a paraglider that would reduce the drag coefficient and, as a whole, a product with improved flight characteristics compared to the current market offer.

2. CHARACTERIZATION

Francis and Gertrude Rogallo's (1951) invention of "kites with completely flexible surfaces" [1] has evolved in two directions. One branch led to the concept of paraglider, a completely flexible parachute-like structure that could be guided and controlled. The other branch led to the concept of hang gliding.

In 1980, Mike Byrne built what is considered to be the first paramotor. Its idea involves the inclusion in the flight assembly a powertrain that generates sufficient traction force to allow the paraglider to take off from any terrain. This model has begun to take shape by designing a frame that can be attached to the paraglider. The frame is designed to contain both the harness to which the pilot is attached and the powertrain.

Paramotors are part of the category of ultralight motorized aircraft. They can be used for training flights, travel flights, leisure flights, search and rescue flights, aerial photography flights or even for sporting purposes, such as acrobatic flight for participation in specific competitions.

The single-seater paramotor assembly has a maximum take-off weight of 250 kg, while the two-seater paramotor assembly has a maximum take-off mass of 400 kg. They fly at speeds of between 25 km/h and 80 km/h, at altitudes of up to 5500 m.

Paramotors consist of paragliders, suspensions and suspension brackets, the pilot harness, the engine and propeller assembly, the frame on which the engine is mounted and the lifebuoy.

3. CONCEPTUAL DESIGN

The aerodynamics of paragliders are very complex, as they involve unstable and turbulent three-dimensional airflows over flexible and deformable limits. There are complex interactions between the structure and the fluid in which it is located, because the shape of the parachute also influences the flow and each other. The main improvement that can be made to paragliders is to increase the lift/drag ratio. This can be achieved by changing the aerodynamic profile in the leading edge area, more specifically by reducing the diameter of the air retention chambers in the leading edge area, and adding an additional resistance structure in the trailing edge area to maintain the ideal shape of the aerodynamic profile at different angles of attack.

3.1 Requirements list

Solving the research topic requires establishing the list of requirements for the paramotor that is illustrated in Figure 1. The main conditions to be satisfied are:

- proper design;
- construction must be of specified materials;
- engine, propeller, instruments and equipment must be of approved type.

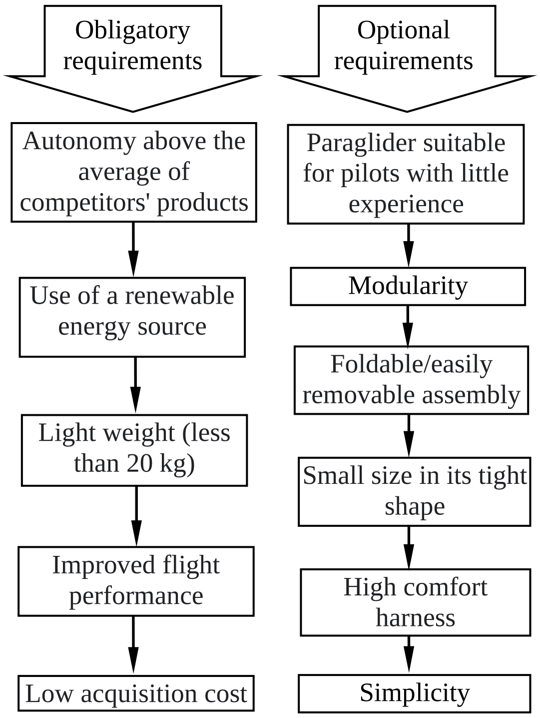

Figure 1 Requirements list [2].

3.2 Constructive aspects

The paraglider is a tire like a wing made of very light material, usually woven from strong synthetic yarns in the form of ripstop (special fabric in which is inserted from place to place a thicker yarn, of higher strength, with a role in stopping the propagation of ruptures by tearing of the surface of the canvas), with a dome-shaped surface, very similar to a modern wing-like parachute, but very different in some respects. Unlike the parachute, when inflated with air, the paraglider takes the form of an aerodynamic profile capable of developing lift. The paraglider consists of two surfaces made of a special material of low porosity connected by membranes that define the profile of the wing, creating a number of caissons through which the air circulates freely. These membranes have "interlocking" holes that allow air to circulate freely between caissons (like honeycombs).

The tire is the only component of the paraglider that produces lift during flight. The tire consists of the upper and lower tissue and forms a semi-rigid lifting surface that is well filled by the current of air that passes through them. The profiling of the cap takes place through cell walls and intermediate walls. The greater their number, the less the surface of the paraglider deviates from the shape of the aerodynamic profile. The lifting cell walls divide the cap into cells, and the non-lifting intermediate cell walls divide it into chambers.

The profile of the paraglider is very important, it being practically the one that imposes the aerodynamic performances. The profile is maintained in flight only due to the pressure that forms inside the cells due to the speed of the air entering and stagnating inside, forming a kind of air cushion with a slightly higher pressure than the airflow on the extrados or intrados (due to the flow, the static pressure decreases, which favors the swelling of the surface).

4. MATHEMATICAL MODELING

The NACA 2412 profile was chosen to obtain the load-bearing surface of the paraglider. Starting from the aerodynamic characteristics of the NACA 2412 profile, the aerodynamic characteristics C_L and C_D of the smooth plane wing (rigid wing with smooth surface) are determined using a MathCAD program.

The lift coefficient on the linear portion of the curve $C_L = f(\alpha)$ is determined by the relation:

$$C_L = C_{L\alpha}(\alpha - \alpha_0) \tag{1}$$

where $C_{L\alpha}$ is the slope of the lift coefficient with incidence α, and α_0 is the incidence where the lift coefficient is zero [3].

The slope of the lift coefficient $C_{L\alpha}$ is determined by the relation:

$$C_{L\alpha} = \frac{C_{L\alpha\, profil}}{1 + \dfrac{57.3 C_{L\alpha\, profil}}{\pi\, e\, AR}} \left[\frac{1}{grad}\right] \tag{2}$$

where e is the OSWALD correction coefficient, and which was considered $e = 1$ due to the fact that the wing is elliptical and the AR is the elongation of the wing.

The drag coefficient $C_D = f(\alpha)$ is determined by the relation:

$$C_D = C_{D0} + C_{Di} \tag{3}$$

where C_{Di} represents the induced drag coefficient and has the expression:

$$C_{Di} = \frac{C_L^2}{\pi AR} \cdot k \tag{4}$$

where k is a correction factor, which has a parabolic evolution as the incidence α increases, therefore, as the lift coefficient C_L increases.

For the smooth flat wing with the geometry shown above, the values resulted: $C_{L\alpha}$=0.07604 1/grad, C_{D0}≅0.01.

Table 1 gives the sizes for $C_L = f(\alpha)$, $C_D = f(\alpha)$ and the fineness $f = C_L / C_D$.

Table 1

Size values for C_L, C_D and f.

α[°]	C_L	C_D	f
-6	-0.304	0.01569	-19.38
-4	-0.152	0.01142	-13.30
-2	0	0.01000	0
0	0.152	0.01142	13.30
2	0.304	0.01569	19.38
4	0.456	0.02287	19.94
6	0.608	0.03302	18.42
8	0.760	0.04629	16.42
10	0.912	0.06282	14.52
11	0.984	0.07321	13.50
12	1.054	0.08420	12.64

13	1.128	0.09915	11.50
14	1.134	0.1117	10.65
15	1.245	0.1269	9.81
16	1.302	0.1463	8.90
17	1.35	0.1687	8.00

Figures 2÷5 show the curves $C_L = f(\alpha)$, $C_D = f(\alpha)$, $C_L = f(C_D)$ for the above conditions. Increasing the angle of attack raises the height of the leading edge above the trailing edge, altering the mass of air acted upon in a given time. Therefore lift and drag increase with larger angle of attack. The working range of angles of attack is from about -6 degree to +17 degree for a normal cambered aerofoil.

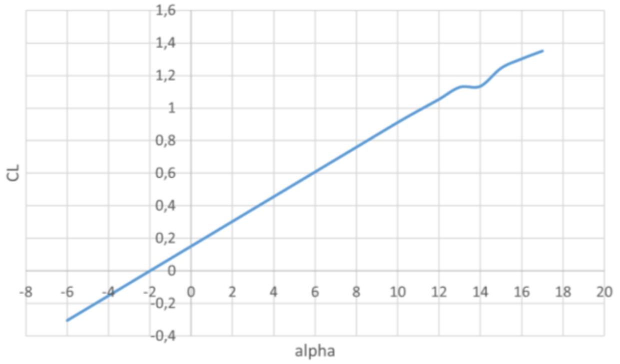

Figure 2 The curve $C_L=f(\alpha)$.

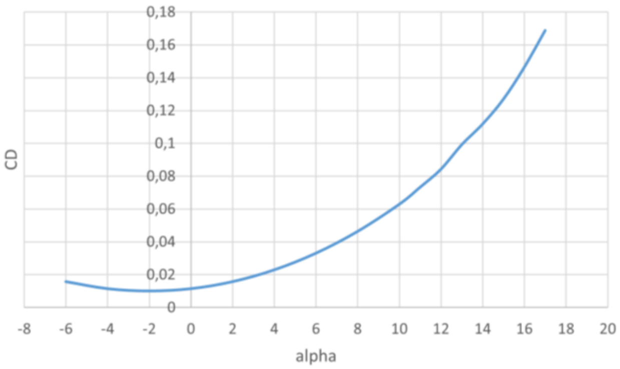

Figure 3 The curve $C_D=f(\alpha)$.

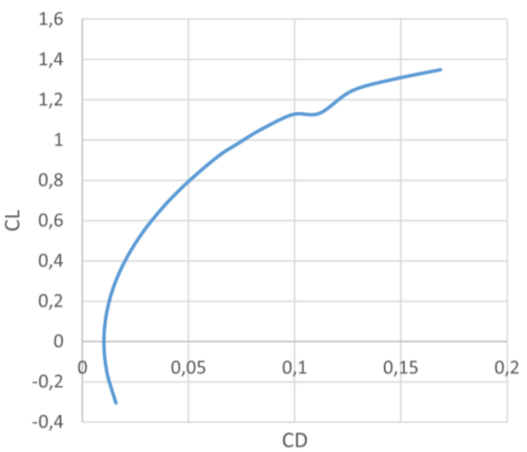

Figure 4 The curve $C_L=f(C_D)$.

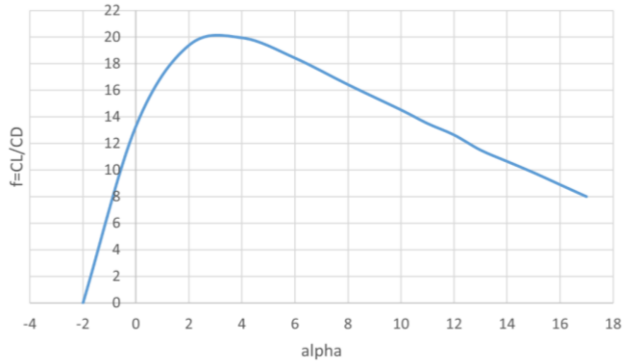

Figure 5 The curve $f=C_L/C_D$.

For the flat wing of the paraglider, which has the attack board cut off to create air circulation inside the volume of the tire, the following estimates have been made:

- the lift coefficient remained the same as for the smooth wing, although there are changes in the C_L, due to the change in the pressure coefficient;
- the zero-lift drag coefficient C_{D0} (profile drag coefficient) changes substantially so that it can vary between $(0.5\ldots 2)C_{D0}$ for the smooth wing.

The following situations were considered:

$$\left(C_{D0}\right)_{1\ paraglider\ wing} = 1.5 \cdot C_{D0\ smooth\ wing} \tag{5}$$

$$\left(C_{D0}\right)_{2\ paraglider\ wing} = 2 \cdot C_{D0\ smooth\ wing} \tag{6}$$

With these assumptions, the values in Table 2 were obtained:

Table 2

C_L, C_D, f values for paragliding wing.

α[°]	C_L	C_{D01}	C_{D02}	f_1	f_2
-6	-0.304	0.02069	0.02569	-14.69	-11.8
-4	-0.152	0.01642	0.02142	-9.257	-7.09
-2	0	0.01500	0.02000	0	0
0	0.152	0.01642	0.02142	9.25	7.10
2	0.304	0.02069	0.02569	14.69	11.83
4	0.456	0.02787	0.03287	16.96	13.87
6	0.608	0.03802	0.04302	15.99	14.13
8	0.760	0.05133	0.05633	14.70	13.50
10	0.912	0.07018	0.07666	13.08	11.90
11	0.984	0.08202	0.08867	12.00	11.10
12	1.054	0.09405	0.10186	11.20	10.30
13	1.128	0.10829	0.11755	10.42	9.60
14	1.134	0.12346	0.13378	9.59	8.85
15	1.245	0.14148	0.15000	8.80	8.80
16	1.302	0.14878	0.17132	8.20	7.60
17	1.350	0.18000	0.19015	7.50	7.10

With these values, the variation curves shown in Figures 6-8 were obtained.

For the flat wing of the paraglider the lift and drag coefficients increase when the angle of attack increases in the working range [-6, 17].

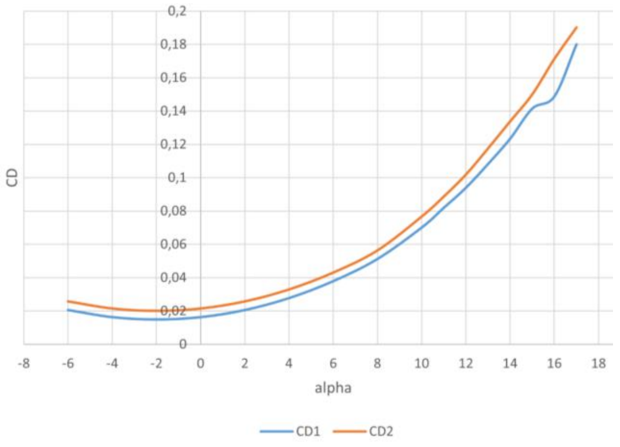

Figure 6 The curve C_D=f(α) with $(C_{D0})_1$ and curve C_D=f(α) with $(C_{D0})_2$.

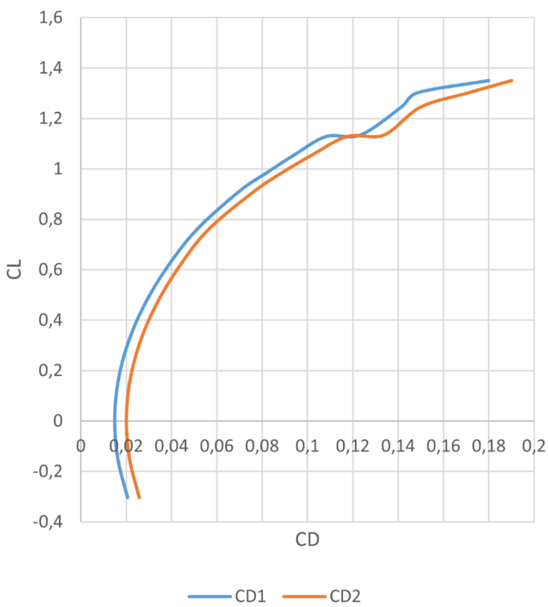

Figure 7 The curve C_L=f(α) with $(C_{D0})_1$ and curve C_L=f(α) with $(C_{D0})_2$.

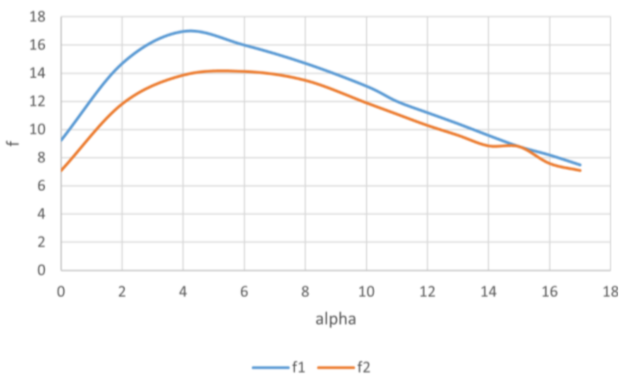

Figure 8 The curve $f_{1,2}$=f(α) for $(C_{D0})_1$ and $(C_{D0})_2$.

Due to the aerodynamic loads, its own weight and the geometric constraints imposed by the suspensions, the wing acquires a vaulted shape (Figure 9). Only tensile forces appear in the veil, and the suspensions give the shape of a circular arc, having a radius R = 7.6 m.

Other geometric features of the wing result:

- the half-angle of the vault opening θ = 0.974 rad = 55.788°;
- projected wing span bp = 12.57m;
- projected wing area Sp = 37.413m^2;
- elongation of the projected wing Ap = 4.233;
- flattening coefficient ap = 11.63% ≅12%.

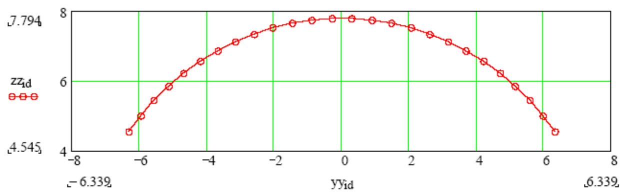

Figure 9 The shape of the vaulted wing.

The front view of the vaulted wing of the paraglider was obtained with a MathCAD program that provided the coordinates of the profile at any point.

For the vaulted wing, the lift coefficient three dimensional C_L =f(α) is determined on the linear portion with the relation:

$$C_L = C^*_{L\alpha}(\alpha - \alpha_0) \tag{7}$$

where:

$$C^*_{L\alpha} = \frac{C_{L\alpha\ profil}}{1 + \dfrac{57.3 C_{L\alpha\ profil}}{\pi A_p}} \cdot \frac{S_p}{S} \tag{8}$$

where A_p = 4.223 is the elongation of the plane projection of the curved wing. Thus, for 12% flattening, $C^*_{L\alpha}$ = 0.06307 1/degree = 3.343 1/rad resulted. The values C_L = f (α) are given in Table 3.

Table 3

C_L = f (α) values for the vaulted wing.

α[°]	C_L	C_{D1}	C_{D2}	f_1	f_2
-4	-0.126	0.01621	0.02121	-7.78	-5.95
-2	0	0.01500	0.02000	0	0
0	0.1262	0.01621	0.02121	7.78	5.95
2	0.2523	0.01987	0.02487	12.70	10.14
4	0.3784	0.02602	0.03182	14.50	12.28
6	0.5046	0.03479	0.03979	14.10	12.68
8	0.6307	0.04605	0.05105	13.70	12.35
10	0.7569	0.06104	0.06687	12.40	11.35
12	0.8830	0.08101	0.08700	10.90	10.15
14	1.0092	0.10568	0.11340	9.55	8.50

Figure 10 shows the variation curve C_L = f(α) obtained with the values given in table 3.

The C_D drag coefficient was calculated with the relation:

$$C_{D_{1,2}} = (C_{D0})_{1,2} + C_{Di} \tag{9}$$

where

$$C_{Di} = \frac{C_L^2}{\pi A_p} \cdot k \tag{10}$$

$$(C_{D0})_{1,2} = 0.015 \div 0.02 \tag{11}$$

are values that are found in the literature [4]. Two values were considered for C_{D0} because there are no definite (experimental wind) data. We consider that the values C_{D01} and C_{D02} ensure the increase of the resistance of the curved wing and fall within the usual range.

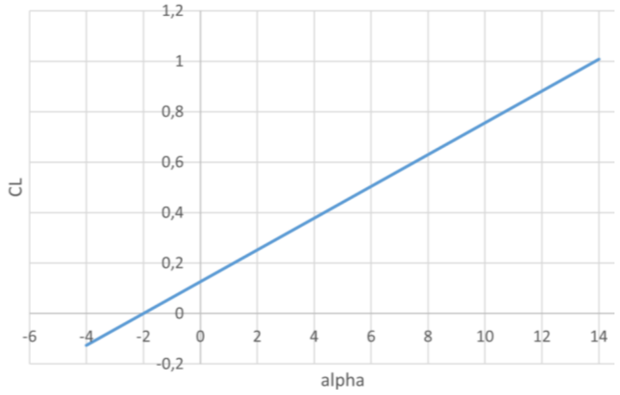

Figure 10 Curve $C_L = f(\alpha)$ for the vaulted wing.

5. IMPROVING PROFILE CHARACTERISTICS

The higher the internal pressure, the better the stability of the veil.

The area of the profile that is perpendicular to the direction of air flow is called the stagnation point. At that point, the airflow separates in two directions, one side will flow on the extrados and the other on the intrados. For a certain flight speed, the pressure reaches a maximum value at the stagnation point. The designer must place the air inlet at the stagnation point in order to obtain an internal pressure value as close as possible to the value PC = 1 (PC-pressure coefficient). However, the stagnation point is not fixed along the profile, but moves according to the angle of incidence.

One way to improve the features is to move the intrados to the bottom, as shown in Figure 11.

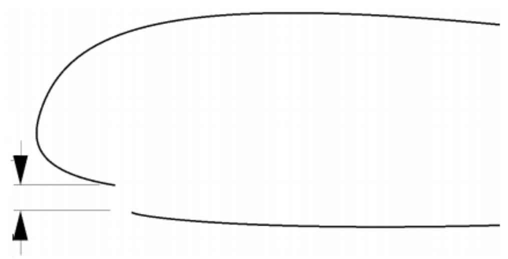

Figure 11 Variant for positioning the air inlet.

This shape of the profile allows sufficient internal pressure to be generated. The disadvantage of this profile is the disturbance of the laminar flow of the air flow; in the case of higher angles of incidence, a turbulent flow is created near the inlet, which decreases the value of the pressure inside the wing.

The solution to this problem is the "Shark Nose" profile [5] obtained by adding a concave part in the usual area of the stagnation point (Figure 12). This concave part will greatly reduce the position range of the stagnation point.

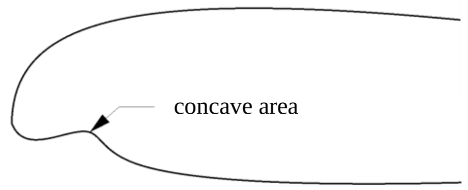

Figure 12 "Shark nose" aerodynamic profile.

This concave part is considered an area where the airflow slows down. It produces the opposite effect of a Venturi tube having a larger area where the air will flow more slowly. The slower the air in this area, the closer the PC value is to 1. An advantage of this concave part is its symmetrical shape which ensures increased pressure both during flight at high angles of attack and at low angles of attack. At the same time, as the range of stagnation points decreased, it was possible to reduce the size of the intake manifold and, therefore, to obtain greater pressure in front of it.

6. 3D MODELLING OF PARAGLIDER AIRFOIL

Paratailor 9 software was used to generate the paraglider model. Paraglider was generated using data from the two MathCAD programs (Figures 13-15).

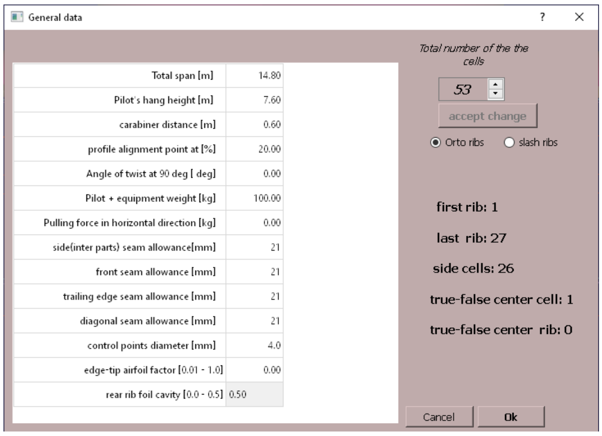

Figure 13 General data.

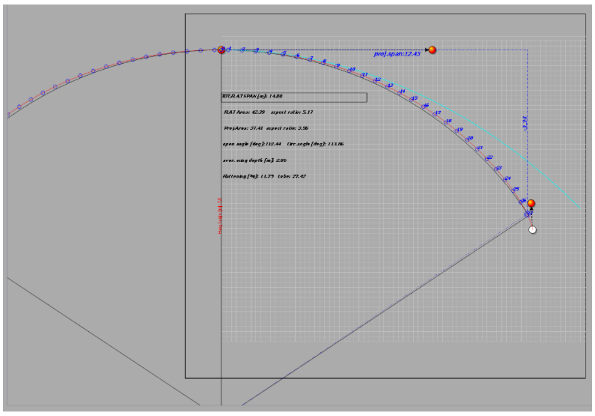

Figure 14 The vaulted shape of the wing.

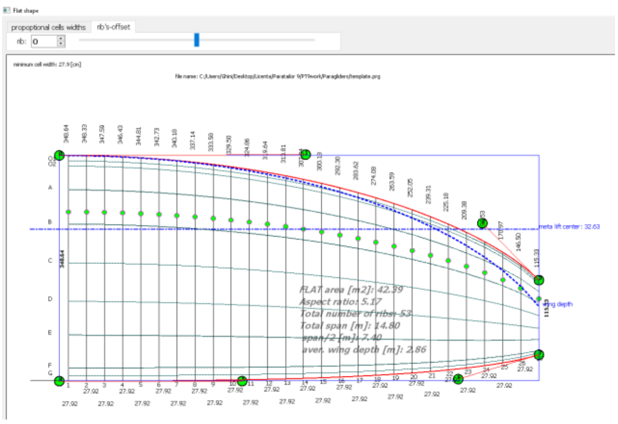

Figure 15 Plane shape of the wing.

To the aerodynamic profile (Figure 16) determined by the points generated by the MathCAD program was added the modification of the attack board using the functions of the Paratailor 9 program.

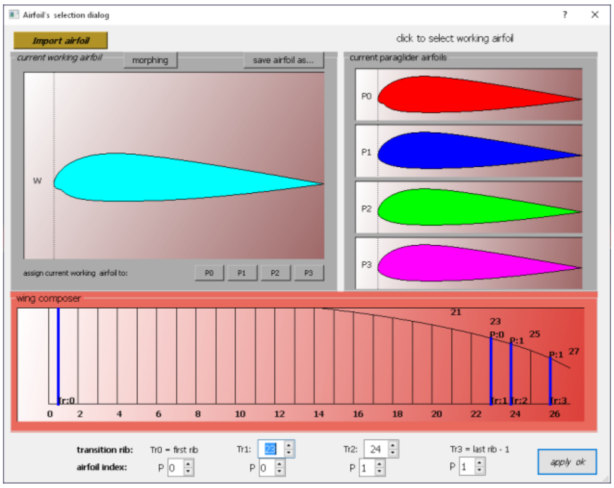

Figure 16 Aerodynamic profile of the paraglider.

Following the introduction of these data, the ribs arranged in the vaulted shape of the paraglider were obtained, which corresponds to the shape during the flight (Figure 17).

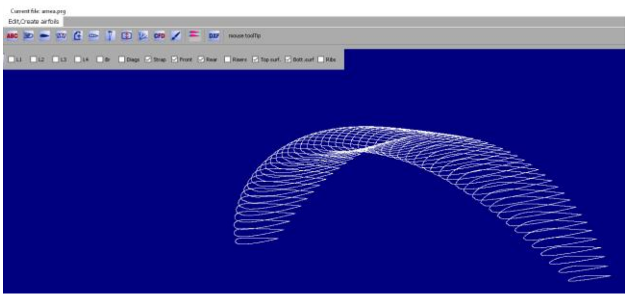

Figure 17 Paraglider ribs.

To ensure the structural integrity of the paraglider, diagonal ribs are needed, arranged between the loaded main ribs. To reduce the weight of the wing without compromising its structural integrity, profiles for the ribs under load will be used.

At the end, the network of suspensions is generated and the paraglider model is obtained (Figure 18).

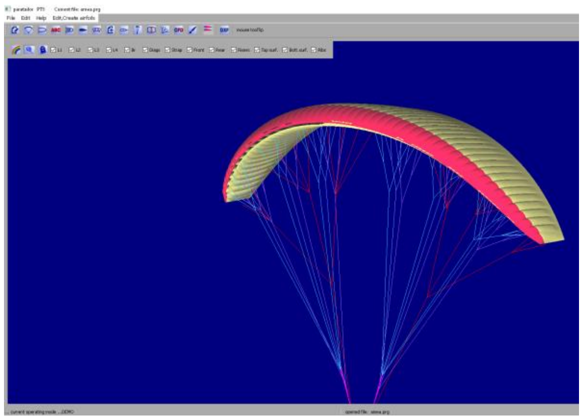

Figure 18 The paraglider model.

7. CONCLUSIONS

The designed paraglider is theoretically analyzed and compared with other paragliders having similar geometric characteristics. Thus, the paraglider obtained complies with the EN B standard (DHS 1-2), being suitable for pilots with little flight experience. Also, the modification of the aerodynamic profile attack board gives the paraglider good maneuverability characteristics at angles of attack at which other paragliders begin to suffer from cell deflation.

Given the features presented, but also the low costs of acquisition, operation and maintenance, the paramotor designed in this paper has achieved all the proposed objectives.

REFERENCES

[1] Rogallo, G.S., Rogallo, F.M. (1951). *Patent: Flexible Kite*, SUA Brevet 2546078.

[2] Dobre, D. (2014). *Dezvoltare de produs-Baze teoretice şi studii de caz*, Editura Bren, ISBN 978-606-610-117-2, Bucureşti.

[3] Stinton, D. (1983). *The design of the aeroplane*, Oxford BSP Professional Books.

[4] Sarthe, J. (1999). *Modélisation d'un parapente*, Université de Savoie.

[5] Abdelqodus, A.A., Kursakov, I.A. (2018). *Optimal Aerodynamic Shape Optimization of a Paraglider Airfoil Based on the Sharknose Concept*, in MATEC Web of Conferences 221, ICDME 2018.

Authors:

Eng. Laurenţiu-Ionuţ CRISTEA, Politehnica University of Bucharest, Faculty of Aerospace Engineering, E-mail: laurionut.cristea@gmail.com

Associate prof. Daniel DOBRE, Ph. D., University Politehnica of Bucharest, Department of Engineering Graphics and Industrial Design, Romania. E-mail: ddobred@yahoo.com